ACS APPLIED MATERIALS & INTERFACES

www.acsami.org

Research Article

A Novel Injectable Piezoelectric Hydrogel for Periodontal Disease Treatment

Lina Roldan, Carolina Montoya, Varun Solanki, Kathy Q. Cai, Maobin Yang, Santiago Correa, and Santiago Orrego*

Cite This: https://doi.org/10.1021/acsami.3c08336

Read Online

ACCESS | Metrics & More | Article Recommendations | Supporting Information

ABSTRACT: Periodontal disease is a multifactorial, bacterially induced inflammatory condition characterized by the progressive destruction of periodontal tissues. The successful nonsurgical treatment of periodontitis requires multifunctional technologies offering antibacterial therapies and promotion of bone regeneration simultaneously. For the first time, in this study, an injectable piezoelectric hydrogel (PiezoGEL) was developed after combining gelatin methacryloyl (GelMA) with biocompatible piezoelectric fillers of barium titanate (BTO) that produce electrical charges when stimulated by biomechanical vibrations (e.g., mastication, movements). We harnessed the benefits of hydrogels (injectable, light curable, conforms to pocket spaces, biocompatible) with the bioactive effects of piezoelectric charges. A thorough biomaterial characterization confirmed piezoelectric fillers' successful integration with the hydrogel, photopolymerizability, injectability for clinical use, and electrical charge generation to enable bioactive effects (antibacterial and bone tissue regeneration). PiezoGEL showed significant reductions in pathogenic biofilm biomass (~41%), metabolic activity (~75%), and the number of viable cells (~2−3 log) compared to hydrogels without BTO fillers in vitro. Molecular analysis related the antibacterial effects to be associated with reduced cell adhesion (downregulation of *porP* and *fimA*) and increased oxidative stress (upregulation of *oxyR*) genes. Moreover, PiezoGEL significantly enhanced bone marrow stem cell (BMSC) viability and osteogenic differentiation by upregulating *RUNX2, COL1A1*, and *ALP*. In vivo, PiezoGEL effectively reduced periodontal inflammation and increased bone tissue regeneration compared to control groups in a mice model. Findings from this study suggest PiezoGEL to be a promising and novel therapeutic candidate for the treatment of periodontal disease nonsurgically.

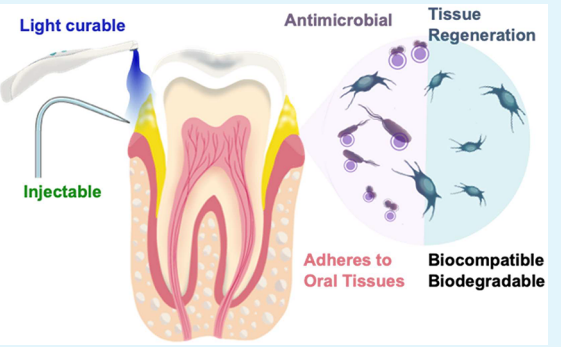

KEYWORDS: *antibacterial, barium titanate, bone regeneration, electrical charges, GelMA, hydrogel, multifunctional, periodontal disease, periodontium, piezoelectric*

1. INTRODUCTION

Periodontal disease (PD) is a major oral disease affecting half of adults in the United States.[1] PD is caused by pathogenic microflora in the biofilm that forms adjacent to the teeth.[2] The bacterial infection induces an inflammatory response that triggers the progressive destruction of the periodontal tissues and, finally, the loss of teeth.[3] The clinical treatment of PD frequently begins with a nonsurgical approach that includes scaling and root planning (SRP) in combination with the administration of adjuvants (local or systemic antibiotics).[4,5] The aim of nonsurgical treatment of PD is to halt the progression of the disease, control infection, and restore gum health without the need for invasive surgical procedures.[6] Nonsurgical treatments are typically the first line of defense in managing PD. However, the clinical success of nonsurgical treatment is only 39%, with major reported inconsistencies, dependence on patient compliance, smoking status, tooth location, and disease severity.[7,8] The SRP plus adjuvant approach has several limitations, including the difficulty to reach pockets with greater depths, limited regeneration of periodontal tissues, limited reduction of the pocket size, and frequent reapplication and long-term use of adjuvants, which raises concerns regarding antibiotic resistance.[9−11] The regeneration of periodontal tissues remains challenging, especially via nonsurgical treatments with moderate/severe conditions and noncompliant patients.[12,13] If nonsurgical treatment is ineffective, surgery may be indicated via bone grafting, guided bone tissue regeneration membranes, and scaffolds that deliver bioactive molecules.[14−17]

Injectable dental biomaterials have gained popularity for the nonsurgical treatment of PD because of their conformability

Received: June 9, 2023
Accepted: August 22, 2023

and facile flowability into the periodontal pocket.[18−21] Specifically, hydrogels are excellent candidates because of their biocompatibility, adhesion, biodegradation, affordability, and simple chemistry.[22,23] Gelatin methacryloyl (GelMA) is a common biomedical hydrogel that has been incorporated with different antimicrobial agents, including zinc, quaternary ammonium, and antibiotics (e.g., ciprofloxacin) for PD treatment.[24−28] Hydrogels enable long-term leaching of the agents with fewer reapplication cycles.[29,30] However, some limitations still exist, including uncontrolled and rapid drug release, microbial resistance build-up, and a lack of complete periodontal tissue regeneration.[31] Ideal hydrogels for PD treatment are expected to not only inhibit bacterial activity to control the inflammatory response but also foster tissue regeneration. The use of multifunctional hydrogels loaded with antibacterial, antioxidant, and/or tissue regeneration agents have been proposed recently.[32] The goal of this approach is to deter bacteria, reduce the imbalance in the redox system, prevent bone resorption, and foster tissue regeneration in the periodontium. For example, a gelatin-chitosan thermosensitive hydrogel was loaded with aspirin and erythropoietin to exert anti-inflammation and tissue regeneration effects, respectively.[33] Periodontal pathogens produce and release chemicals that activate the innate immune system to release proinflammatory cytokines contributing to the progression of the disease.[34,35] To terminate alveolar bone resorption and resolve PD, simultaneous antibacterial and tissue regeneration effects are required. To the best of our knowledge, this approach is limited in the existing nonsurgical treatment options for PD.

Piezoelectric materials produce electrical charges in response to external vibrations and mechanical stimulation.[36] These materials have been extensively used for energy harvesting devices, sensors, and medical applications.[36,37] For example, piezoelectric polymers have been used for orthopedic bone tissue regeneration by promoting osteogenic proliferation and differentiation due to their electromechanical properties.[38] Barium titanate ($BaTiO_3$, BTO) is a biocompatible piezoelectric ceramic that has gained substantial interest in recent years due to accepted biocompatibility, high dielectric constant, excellent ferroelectric properties, and the possibility of nanoparticle fabrication.[39,40] These qualities have pushed BTO as a prime candidate for the development of biomedical technologies and wearable bioelectronics. Piezoelectric materials have recently been used in dentistry for antimicrobial, remineralization, and tissue engineering applications.[41,42] For example, we developed a piezoelectric resin composite after mixing BTO fillers with a standard resin matrix. This material prevented the formation of carries-related biofilms after showing a 3 log reduction on the bacterial load.[42] In a different study, BTO fillers were added into PMMA to enable antifungal effects that prevented denture-related pathogenic biofilms.[43] These studies attributed the antimicrobial mechanism to reactive oxygen species (ROS) production and oxidative stress. Despite the many advantages of BTO, the antimicrobial effects against periodontal pathogens and periodontal tissue regeneration have not been elucidated.

In this study, we developed an injectable multifunctional piezoelectric hydrogel incorporated with BTO fillers (PiezoGEL) for the nonsurgical treatment of PD. The new biomaterial offers a unique combination of antibacterial and bone tissue regeneration effects. Using a minimally invasive probe, PiezoGEL can be locally injected into an infected periodontal pocket and light-cured to form a graft in situ. PiezoGEL is a minimally invasive treatment that removes pathogens from the periodontal pocket without using drugs. In addition, the same biomaterial system promotes alveolar bone tissue regeneration in the periodontium. Particularly, in this study, we evaluated both the antibacterial and bone tissue regeneration effects for periodontal disease treatment, both in vitro and in vivo.

2. MATERIALS AND METHODS

2.1. Fabrication of Piezoelectric Hydrogels. PiezoGEL was fabricated by mixing 200 mg/mL GelMA (Advanced Biomaterials, 5208) with 9 mg/mL silanized particles of BTO (US Nanomaterials, US3830, 200 nm) and sterile phosphate-buffered saline (PBS) (SI-1 in Supporting Information). This filler size offered an appropriate balance between the injectability and electrical charge generation. Increasing this particle size would increase the hydrogel viscosity and injection force and lower the degradation rate. The photoinitiator lithium phenyl-2,4,6-trimethylbenzoyl phosphonate (LAP) (Advanced Biomaterials, 5269) was added at a proportion of 0.35% wt of the solubilized GelMA. Lyophilized GelMA and PBS (70 °C) were mixed using a vortex mixer (Daigger Vortex-Genie) until GelMA was fully solubilized. BTO particles were added during the continuous shaking of the mixture. Subsequently, LAP was dissolved in 100 μL of warm PBS (70 °C) and mixed with the dissolved GelMA/BTO mixture. Control hydrogels were prepared without BTO filler (GelMA). The mixture was poured into a 6 mL polypropylene syringe, which was used as a mold for the uncured solution. After placing in the syringe, a 405 nm visible light was positioned at 1 cm of the solution and irradiated for 2 min, resulting in a total radiant exposure of 24.5 J/cm^2. After curing, the samples were carefully demolded, cut into cylinders (12 mm diameter and 6 mm thickness), and stored in DI water for 24 h at 4 °C for the release of unreacted monomers. The hydrogels were prepared inside a biological safety cabinet and sterilized using a UV lamp (254 nm) for 15 min before each test. Samples were placed 30 cm from the UV source.

2.2. Physical, Mechanical, and Electromechanical Characterization of Hydrogels. We evaluated the physical, mechanical, and electromechanical properties of PiezoGEL, including the surface pore size (SI-2), surface roughness (SI-3), rheology, injectability, and biodegradation.

Rheological properties of the hydrogels were assessed using a Rheological StressTech HR rheometer (ATS RheoSystems) with parallel plate geometry (25 mm diameter and 1 mm gap) and samples maintained at 37 °C.[18] The storage and loss moduli of the cured hydrogels were measured by conducting a strain sweep from 0.01% to 500% at 5 Hz with a conditioning time of 3 s, sampling time of 3 s, and 10 points/decade. This is the standard protocol for measuring the rheology of hydrogels for clinical applications.[44] To determine the curing time, rheological tests were performed with 200 μL of uncured GelMA while the liquid mixture was cured using a lamp. Changes in the storage modulus during polymerization were measured as previously described.[44,45]

Injectability was measured by placing 500 μL of a liquid mixture of GelMA or PiezoGEL in a disposable syringe (1 mL) connected to a 20-G$^1/_2$ tip without air bubbles. The syringe was placed in a rig coupled to a universal testing machine (Electroforce 5500).[46] The machine cross-head was used to push the syringe plunger and simulate an extrusion flow rate of 2 mL/h (cross-head of 0.45 mm/s). The force applied to the plunger during injection was recorded.

Hydrogels' voltage/electrical charge generation was measured by placing electrodes (thin copper sheets) on the top and bottom surfaces of the cured hydrogels. The electrodes were connected to a piezoelectric amplifier (TE Connectivity Piezo Film Lab Amplifier) to measure the open-circuit voltage. The hydrogels were then cyclically loaded using a universal testing machine, following a sinusoidal waveform (3 N, 2 Hz). The voltage was recorded during the stimulation.

The degradation of the hydrogels was performed after preparing the disks (12 mm diameter and 6 mm thickness) and placing them in

https://doi.org/10.1021/acsami.3c08336
ACS Appl. Mater. Interfaces XXXX, XXX, XXX−XXX

DI water for 24 h. Subsequently, the disks were dried under a vacuum until they reached a constant weight and then submerged in PBS (pH 7.4) for 14 days at 37 °C. The medium was refreshed every day. Dry weight loss was monitored as a function of time (0, 7, and 14 days). Weight loss (ΔW%) was calculated as the change in weight (initial − final)/(initial).[47] For all evaluations, three samples from independent batches were evaluated.

2.3. Antibacterial Evaluation in Vitro. *2.3.1. P. gingivalis Biofilm Model.* To evaluate the antibacterial effects of the hydrogels, we used a single-species biofilm model following our established protocols.[42] *P. gingivalis* was used as the test bacterium because it is the most important pathogenic bacterium in chronic PD.[48,49] This pathogen produces lipopolysaccharides that induce proinflammatory cytokines/chemokines that cause bone loss.[50] The strain ATCC 33277 was plated on prereduced sheep blood agar supplemented with hemin (5.0 g/mL) and menadione (0.5 g/mL) and incubated under anaerobic conditions (5% H_2, 5% CO_2, 90% N_2) for 4 days at 37 °C.[51] To create the bacterial liquid culture, a single colony was harvested and incubated anaerobically overnight in reduced/stirred-supplemented brain heart infusion (BHI). The solution was diluted in BHI to obtain OD 600_{nm} = 0.1 (~1×10^8 cells/mL). Sterile-cured hydrogels were submerged in 3 mL of bacterial culture and subjected to cyclic loading (Cell Scale MechanoCulture TX) throughout the incubation period (24 h). During the experiment, the load magnitude was adjusted from −0.5 to −3 N, resembling the clinical stress in the periodontium (~0.90 MPa, frequency of 2 Hz).[52,53] Static hydrogels were also used. After incubation, the top and bottom of the hydrogel were cleaned with a blade. Samples (N = 3 per group per evaluation) were gently rinsed with PBS to remove unattached cells and used to evaluate biofilm formation.

2.3.2. Microbiological Biofilm−Biomaterial Evaluations. To assess the biomass, metabolic activity, and a number of viable cells in the biofilms, crystal violet (CV), [3-(4,5-dimethylthiazol-2-yl)-2,5-diphenyltetrazolium bromide] (MTT) assay and counting of colony-forming units (CFU) were performed according to previously established protocols.[42,54] To visualize and quantify live and dead bacteria on the hydrogels, the cells were stained by using the LIVE/DEAD BacLight viability kit (Thermo Fisher L7007). Briefly, the hydrogels were placed in 1 mL of PBS and vortexed for 1 min to detach the biofilm. Cells were collected by centrifugation (12 *g* for 5 min at room temperature) and stained with a fluorescent stain composed of 3 μL of SYTO9 and 3 μL of propidium iodide (PI) dissolved in 1 mL of ultrapure water (final concentration 6 μM for SYTO 9 and 30 μM for propidium iodide). Aliquots (50 μL) of the stain were applied to the bacterial pellets, and the pellets were incubated in the dark for 20 min. The bacterial pellet was gently rinsed with filter-sterilized water to remove excess dye. The cells were imaged using a confocal laser scanning microscope (CLSM) (Olympus Corporation, FV1200). Five experimental images were obtained for each sample. All intensities were corrected for background fluorescence and captured using identical settings. The numbers of live and dead bacteria were quantified using ImageJ software (SI-4).

2.3.3. Molecular Biofilm−Biomaterial Evaluations: RNA Extraction and Gene Expression Assays. Total RNA was extracted from biofilms after 24 h of incubation using the RNeasy Mini Kit (QIAGEN) according to the manufacturer's instructions. The RNA yield and quality were assessed using a NanoDrop instrument (Thermo Fisher Scientific). cDNA synthesis was performed using the RT^2 First Strand Kit (Qiagen, Hilden, Germany) according to the manufacturer's protocol. For cDNA synthesis, 100 ng of RNA was used. Reverse transcription quantitative polymerase chain reaction (RT-qPCR) was performed by using a Bio-Rad CFX96 thermocycler (Bio-Rad, USA) and an iTaq Universal SYBR Green Supermix (Bio-Rad, USA). Gene-specific primers associated with pathogenicity and biofilm formation were used, including *fimA*, *porP*, and *oxyR* (Thermo Fisher Scientific)[55] (SI-5). 16s rRNA was used as the housekeeping gene.[56] RT-qPCR was performed as follows: initial denaturation at 95 °C for 30 s, followed by 40 thermal cycles at 95 °C for 10 s and 60 °C for 30 s. Gene expression was normalized using the comparative C_t ($\Delta\Delta C_t$) method.[57] Each experimental group and gene primer were analyzed in triplicates.

2.4. Bone-Tissue Regeneration Evaluation in Vitro. *2.4.1. Cell Culture and Seeding.* Bone marrow-derived mesenchymal stem cells (BMSCs) were purchased from ATCC (PCS-500-012) and cultured in stem cell basal medium (PCS-500-030) supplemented with stem cell growth medium (PCS-500-040), penicillin, streptomycin, and amphotericin (PCS-999-002). BMSCs were used because they are the most common cell source for bone tissue regeneration and have demonstrated the ability to regenerate periodontal tissue.[58] The cells were incubated at 37 °C and 5% CO_2 in a humidified incubator. In this case, static hydrogels were cured directly in 12-well plates (22.5 mm diameter and 1 mm thickness). The cells were passaged at an 80% confluence. At passage three, cells were seeded at a density of 50 000 cells/cm^2 in 3 mL of media. The hydrogels were then incubated, and cyclic loading (−0.5 to −3 N at 2 Hz) was initiated for the duration of the test (as presented in section 2.3.1). A group of cells were supplemented with an osteocyte differentiation toolkit (PCS-500-052) and used as the positive control (SI-6). A group of cells was seeded in the well plate without hydrogel as a reference. The medium was changed every 48 h. After 7 and 14 days of culture, the cells were evaluated for viability, gene expression, and mineralization.

2.4.2. Cell Viability Test. Cellular metabolic activity was assessed using alamarBlue (Invitrogen A50100).[59] After 7 and 14 days of incubation, the medium was removed (N = 3 samples per group), and 10% (v/v) alamarBlue was added. The plates were incubated for an additional 4 h. Next, aliquots of the solution (100 μL) were transferred to a 96-well plate. Absorbance at 570 nm (A_{570} to detect oxidized alamarBlue) and 600 nm (A_{600} to detect reduced alamarBlue) was measured to calculate the reduction of alamarBlue as instructed by the manufacturer.[59] To estimate the cell viability, the alamarBlue reduction values were normalized by the readings obtained from wells containing only cells as a baseline measurement.[60]

2.4.3. Molecular Evaluation of Bone Regeneration: RNA Extraction and Gene Expression Assays. The hydrogels with the cell monolayer were transferred to a 50 mL centrifuge tube. Direct cell lysis was performed using 600 μL of RTL buffer containing 1% (v/v) β-mercaptoethanol (RNeasy Mini Kit, Qiagen), followed by vortexing for 1 min.[61] RNA was extracted from the resulting cell lysate, followed by cDNA synthesis and RT-qPCR analysis as described in section 2.3.3. Gene-specific primers associated with osteoblast differentiation were analyzed, including *ALP*, *COL1A1*, and *RUNX2*. *GAPDH* was used as the internal control[62] (SI-7). Gene expression was normalized using the comparative C_t ($\Delta\Delta C_t$) method.[57] Each experimental group and gene primer were measured in triplicates.

2.4.4. Mineralization Assay. Mineralization was measured on day 14. First, the cells were fixed with 4% formalin for 15 min at room temperature and stained with Alizarin Red S (ARS) (40 mM, pH 4.2) (ScienCell), followed by incubation at 37 °C for 10 min.[63] The stained samples were diluted with 800 μL of 10% (v/v) acetic acid and neutralized with 200 μL of 10% ammonium hydroxide for 30 min. Optical density was measured at 405 nm (A_{405}) using a Multiskan SkyHigh spectrophotometer. Before the experiment, a calibration curve was constructed to validate ARS measurements[64] (SI-8). The absorbance results were normalized to the cell growth area within the hydrogels, and each experimental group was evaluated in triplicates.

2.5. Periodontal Bone-Tissue Regeneration and Inflammatory Evaluations in Vivo. *2.5.1. Animals and Procedures.* The treatment of PD using PiezoGEL was evaluated using an established ligature-induced mice model.[33,65,66] All animal experiments were reviewed and approved by the Institutional Animal Care and Use Committee (IACUC) at Temple University (Protocol 5063) and complied with institutional, state, and federal policies. Female C57BL/6 mice (N = 20) (Charles River Laboratories, Malvern, USA) weighing approximately 25 g (8−12 weeks of age) were obtained. To induce PD and bone loss, animals were anesthetized with 4% (v/v) isoflurane. A 5−0 silk ligature (Roboz Surgical Instrument, SUT151) was tied around the left maxillary second molar for 8 days[67] (Figure 4a). To initiate treatment, animals were

https://doi.org/10.1021/acsami.3c08336
ACS Appl. Mater. Interfaces XXXX, XXX, XXX−XXX

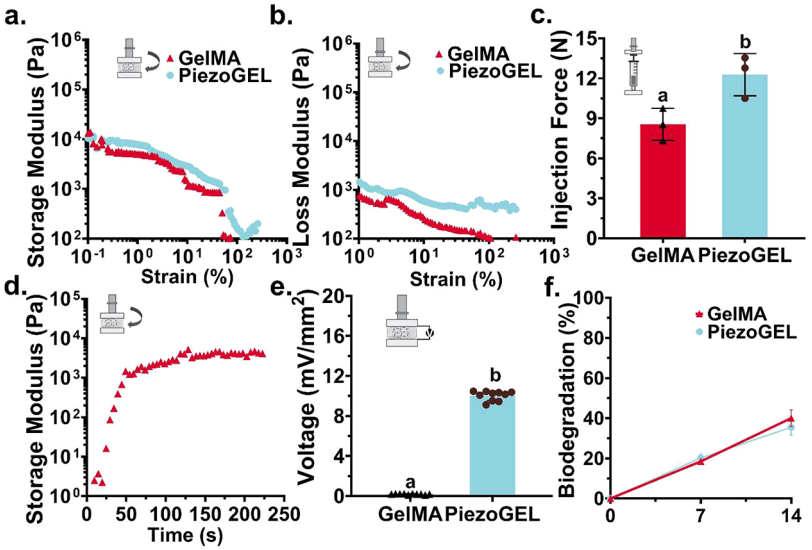

Figure 1. Characterization of GelMA and PiezoGEL hydrogels. (a) Storage modulus and (b) loss modulus of cured hydrogels as a function of strain. (c) Injection force required for the uncured hydrogel to be extruded through a 20-G$^{1}/_{2}$ tip. (d) Storage modulus of GelMA hydrogel as a function of the time. Indication of polymerization. Measurements were performed at 37 °C. (e) Voltage per surface area generated after being subjected to a cyclic compression load of 3 N at 2 Hz. (f) Biodegradation profiles of hydrogels placed in phosphate buffered saline (PBS) for 14 days at 37 °C. Mean values with different letters are significantly different from each other ($p \leq 0.05$).

anesthetized with 4% (v/v) isoflurane. Clinical examination was performed by measuring the probing pocket depth using a Williams probe. Five mice were randomly assigned to each experimental group, positive control (Healthy), PiezoGEL, GelMA, and SRP. Four animals were included in the no treatment group. Before treatment, SRP was performed inside the defect using a dental Gracey Curette (Micro Mini Five #18). The hydrogels were carefully injected into the periodontal defect using a micropipet containing approximately 10 μL of the uncured hydrogel. Then, the hydrogel was cured for 20 s using a 405 nm visible light positioned at 1 cm from the material (total radiant exposure of 3.1 J/cm^2). After one month of treatment, the mice were euthanized by CO_2 inhalation. Collected tissue samples were fixed in 10% formalin for 24 h at 4 °C and subsequently transferred to 80% ethanol for further analysis according to established protocols.[66]

2.5.2. Periodontal Bone-Tissue Regeneration Assessment. Two methods were used to assess the bone tissue regeneration performance. First, the probing pocket depth (PPD) was measured before and after treatment by using a periodontal probe. The change in pocket depth was calculated by subtracting the before and after treatment measurements and normalized to the initial defect depth (day 0). Second, microtomography (micro-CT) was used to obtain a 3D reconstruction of periodontal hard tissues and measure the changes in bone tissue. Briefly, the fixed maxillae were scanned using a scanner (Bruker Skyscan 1172 XR) operated at an accelerated potential of 65 kV, a beam current of 156 μA, an exposure time of 430 ms, and an imaging resolution of 18 μm. All scans were aligned along the sagittal, transverse, and coronal planes, ensuring that all images had a consistent orientation (Data Viewer software). The scanned DICOM images were reconstructed into a 3D image (Nrecon software). Micro-CT reconstruction was analyzed according to established protocols.[68] The brightness and contrast of all images were adjusted through histogram standardization (0.00−0.15) to enhance accuracy and enable automated algorithmic analysis and image comparison.[69] To assess the amount of regenerated bone tissue, the standard distance between the CEJ and ABC between M1 and M2 (defect location) was measured.[66] To assess the regenerated bone tissue volume, we measured the percentage of bone tissue in selected areas over four planes spaced by 90 μm along the occlusal/apical direction.[70] Each selected area (100 × 300 μm^2) was consistently analyzed between M1 and M2. The percentage of bone tissue of each area and plane was added. A healthy mouse with no defect or disease was considered as 100% for comparison.

2.5.3. Histological Assessment. The maxillae were decalcified in 25% formic acid for 48 h after fixation. Samples were embedded in paraffin, and 5 μm thickness sections perpendicular to the long axis of the teeth were obtained. Histological sections were stained with hematoxylin−eosin (H&E) and examined by light microscopy (Nikon Eclipse 50i microscope). The slides were digitally scanned using the ScanScope CS system (AperioScan Technologies, Vista, CA, USA) and ImageScope viewing software. Histological measurements included blood vessel count, erythrocyte count, epithelial length (SI-9), lymphoplasmacytic infiltration, and congestion[71,72] (SI-10).

3. STATISTICAL ANALYSIS

For all evaluations, statistical differences were determined using one-way analysis of variance (ANOVA) with a significance level of 0.05. The ANOVA assumption of normal distribution was assessed by the Shapiro−Wilk test, and the assumption of homoscedasticity was assessed using Levene's test. Tukey's post hoc test was used for multiple comparisons with a 95% confidence level. Statistical analyses were performed using GraphPad Prism 9 software (GraphPad Software, California, USA). Samples for three different batches were used for experimentation.

4. RESULTS AND DISCUSSION

4.1. Hydrogels Characterization. Overall, the rheological evaluations showed that adding BTO to GelMA did not significantly affect the loss and storage modulus (Figure 1a,b). Shear-thinning behavior was observed for the two formulations (GelMA and PiezoGEL). Such behavior is ideal for clinical application since it facilitates the manipulation and delivery of the hydrogel into the periodontal pocket. A similar storage modulus (10^4 Pa) was measured for both hydrogel formulations in the linear region of the curve (Figure 1a). For the loss modulus, at lower strain rates, the incorporation of BTO did not affect the viscous behavior (10^3 Pa). At higher strain rates, PiezoGEL exhibited a higher loss modulus compared to GelMA (Figure 1b). A storage modulus of 10^4

https://doi.org/10.1021/acsami.3c08336
ACS Appl. Mater. Interfaces XXXX, XXX, XXX−XXX

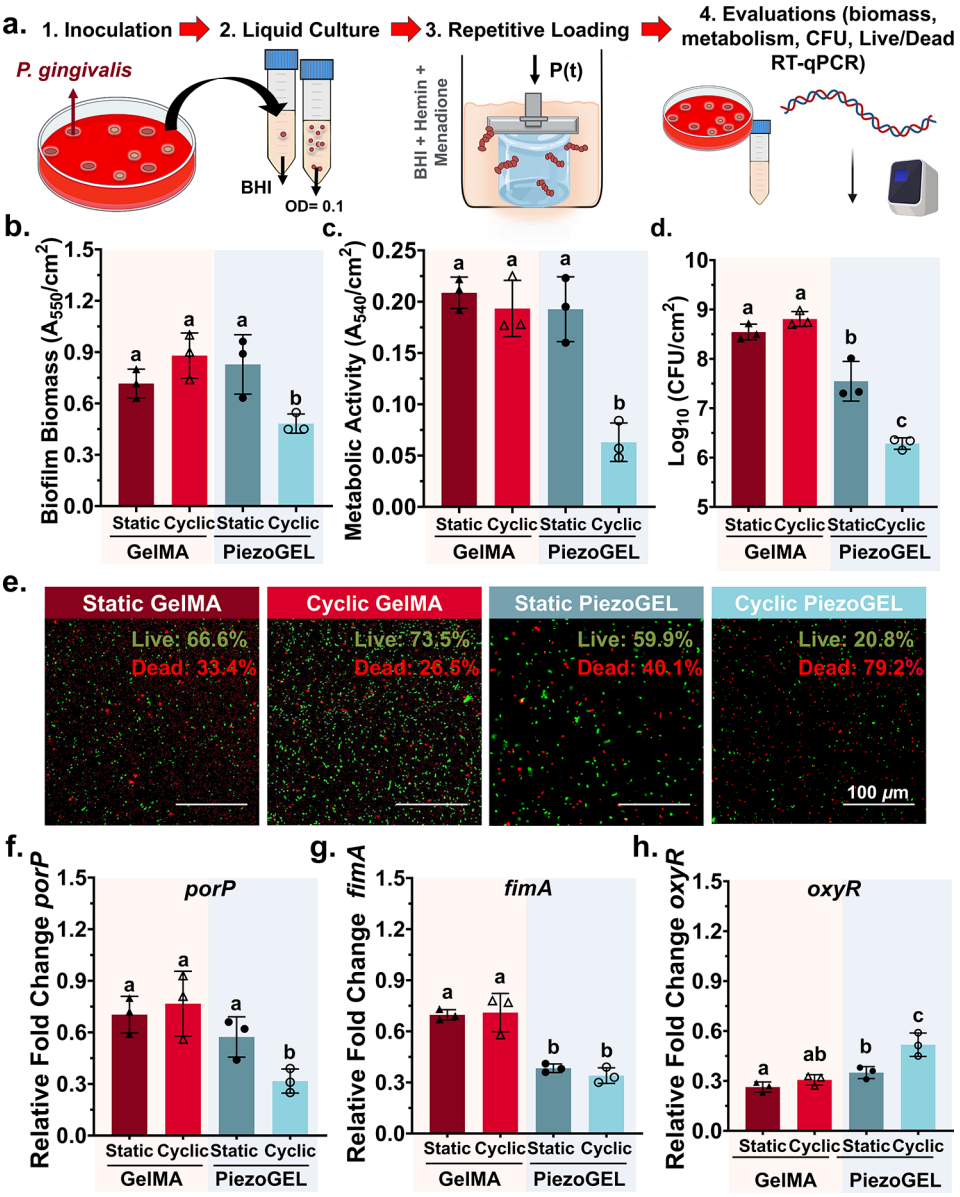

Figure 2. Antibacterial evaluation of GelMA and PiezoGEL hydrogels against *Porphyromonas gingivalis* in vitro (a) Schematics of the model used to cultivate biofilms on hydrogels subjected to cyclic mechanical loading and static (no load). Microbiological evaluations measuring (b) biofilm biomass, (c) metabolic activity, and (d) cell viability (or colony forming units (CFU)). (e) Representative CLSM images of *P. gingivalis*. Cells were stained with Syto-9 (green) and propidium iodide (red) to indicate live and dead bacteria, respectively. Changes in the expression of selected genes related to *P. gingivalis* biofilm formation: (f) *porP* encoding biosynthesis of cell-surface polysaccharides and biofilm growth, (g) *fimA* related to the adhesion of host−pathogen interactions, and (h) *oxyR* regulator of oxidative stress. The relative gene expression was normalized to 16S rRNA levels (housekeeping). Mean values with different letters are significantly different ($p \leq 0.05$).

Pa offers a hydrogel with proper mechanical support and stability to periodontal tissues, while a loss modulus of 10^3 Pa can absorb mechanical forces aiding tissue healing and reducing stress concentration.[73] To further explore the injectability, we measured the force required to push the plunger of a syringe and extrude the material. Using a syringe connected to a 20-G tip, we observed that GelMA and PiezoGEL hydrogels had an average injection force of 8.5 N (0.9 kgf) and 12 N (1.2 kgf), respectively (Figure 1c). The increase in injection force with the addition of BTO was expected because the ceramic fillers increase the viscosity of the solution and add restriction during needle extrusion.[19] Nonetheless, the injection force for PiezoGEL is acceptable for the clinical use (<3 kgf).[18] Real-time photorheological tests were performed to determine the curing times of the hydrogels. Appropriate polymerization reduces cytotoxicity due to the leaching of unreacted monomers or residual photoinitiators and guarantees mechanical stability.[74] The change in the storage modulus with time of PiezoGEL is presented in Figure 1d. Results showed a typical polymerization curve with a step increase in the first 50 s and reaching a plateau after 120 s of light exposure.[75] We also evaluated the voltage produced by the hydrogels after stimulation with cyclic mechanical loading, which is necessary to produce electrical charges and enable the bioactive effects. The PiezoGEL produced ~10 mV/mm^2 under a stimulation of 0.9 MPa (Figure 1e), which is a stress magnitude found in a clinical setting. As expected, no voltage was produced in the control

https://doi.org/10.1021/acsami.3c08336
ACS Appl. Mater. Interfaces XXXX, XXX, XXX−XXX

GelMA (Figure 1e). Furthermore, the biodegradation of the hydrogels under physiological conditions (PBS) was also evaluated. Hydrogels used for PD treatment must degrade to "open up" space for the regeneration of new tissue and the reduction of the pocket size.[19] The degradation profile showed a maximum degradation of ~40% for both formulations after 14 days of evaluation (Figure 1f). No significant differences were observed between the groups on days 7 and 14. Since the quantity of BTO with respect to GelMA is small, the biodegradation profiles are expected to be similar. The degradation profile of GelMA can be influenced by different media types, including aqueous solutions, enzymatic solutions, and simulated body fluids.[76] Enzymatic solutions, such as collagenases, provide accelerated degradation rates, whereas simulated body fluids can provide a more realistic assessment of the hydrogel's stability and degradation rate in vivo.[78,79]

4.2. Antibacterial Evaluation in Vitro. The antibacterial activity of PiezoGEL was assessed against *P. gingivalis*, a crucial pathogen involved in the development of PD. For these evaluations, hydrogels were subjected to static (no load) and cyclic (repetitive) loading to enable electrical charge generation during the incubation period (Figure 2a). The hydrogel−bacteria interactions were evaluated by measuring biofilm biomass and metabolic activity and by counting the number of viable cells (CFU). For biofilm biomass, no significant differences were observed in the GelMA hydrogels regardless of the loading condition and the static PiezoGEL (Figure 2b). However, PiezoGEL stimulated with cyclic loading showed the lowest biofilm biomass. Similar results were obtained for the metabolic responses of the biofilms (Figure 2c). The lowest reduction was observed in the cyclic PiezoGEL group. These findings suggest that when PiezoGEL activates the electrical charge production via cyclic loading, antibacterial effects are enabled. Regarding CFU, our results showed that most bacteria were found in the GelMA groups (Figure 2d and SI-11), suggesting that GelMA did not have any antibacterial effect. A significant reduction in viable cells was observed for static PiezoGEL (~1 log reduction). However, PiezoGEL stimulated by cyclic loading (charge regeneration) resulted in a 2−3 log reduction (Figure 2d). Regardless of the mechanical loading conditions, PiezoGEL exhibited a reduction of the bacterial load. These findings were validated by imaging live and dead cells attached to hydrogels (Figure 2e). The highest number of live cells (green) was observed in the GelMA groups (66−73%). Conversely, cyclic PiezoGEL treatment resulted in the highest number of dead cells (~79%) and the lowest number of live cells. Our results confirm and extend previous findings showing the antimicrobial effect of piezoelectric charges on oral pathogens.[42,43,77]

To reveal the antibacterial mechanism and understand changes in biofilm formation, we measured the expression of genes related to adhesion, biofilm formation, and virulence. First, we measured the expression of *porP*, which encodes the biosynthesis of cell-surface polysaccharides, biofilm growth, and gingipain translocation.[48] Our results showed that *porP* was significantly downregulated for the cyclic PiezoGEL compared with the other groups (Figure 2f). It is known that under normal biofilm growing conditions, *porP* is upregulated[48] suggesting that cyclic PiezoGEL altered the adhesion potential to biomaterial surfaces. Second, we measured the relative gene expression of *fimA*, a gene responsible for encoding the major subunit protein of fimbriae. *fimA* is related to bacterial colonization and adhesion, and its primary role is to promote bacterial attachment to oral surfaces.[78] Under normal growth conditions, *P. gingivalis* expresses high levels of *fimA*, optimizing adherence to available substrates.[79] Our results show a significant downregulation of *fimA* in the PiezoGEL group regardless of the loading condition (static or cyclic) (Figure 2g). Previous studies have associated decreased expression of *fimA* with inhibition of the initial attachment of *P. gingivalis* to the tooth surface and, therefore, the subsequent formation of biofilm and maturation.[78] The downregulation of *fimA* in PiezoGEL indicates a reduced amount of biofilm, which is consistent with microbiological findings, such as the reduced cell count (CFU) (Figure 2d). Third, we evaluated changes in *oxyR* since this gene has been associated with an oxidative stress regulator sensitive to hydrogen peroxide.[80,81] *OxyR* is crucial for *P. gingivalis*' aerotolerance and plays a significant role in regulating other vital virulence factors such as biofilm formation.[82] Previous studies have proposed ROS as the antibacterial mechanism triggered by (piezo)electric charges.[83] During the normal respiration of obligatory anaerobes, ROS are produced in the respiratory electron transport chain and cytoplasm.[84] Without an ideal redox balance, overproduced ROS can damage essential biological macromolecules, including lipids, proteins, RNA, and DNA.[85] Our results showed a significant increase in the expression of *oxyR* in the cyclic PiezoGEL group compared with the other hydrogel groups (Figure 2h). This suggests ROS as the antibacterial mechanism of PiezoGEL. This finding agrees with our similar studies regarding the antimicrobial mechanism of piezoelectric charges.[42,43,86] As expected, the lowest expression of *oxyR* was observed in GelMA hydrogels, since no electrical charges are produced. The highest expression of *oxyR* in the cyclic PiezoGEL agreed with the maximum reduction in metabolic activity and the number of viable cells (Figure 2c,d).

Overall, the results of this study indicate that the electrical charges produced by PiezoGEL enable antibacterial effects against *P. gingivalis*. We observed a significant reduction in biofilm biomass (~41%), metabolic activity (~75%), and the number of viable bacteria in the biofilm (~2−3 log) compared to hydrogels without charges and BTO fillers. Molecular changes in specific genes suggest that the reduction in biofilm formation and cell viability is related to diminished cell adhesion (i.e., downregulation of *porP* of *fimA*) and oxidative stress (i.e., upregulation of *oxyR*). In this work, we used a single-species model to show the antibacterial effects. Studies have shown that removing virulence factors of *P. gingivalis* from periodontal pockets can significantly reduce the inflammatory response and promote bone regeneration, leading to improved periodontal health.[87] The toxin (lipopolysaccharide) induces the production of proinflammatory cytokines/chemokines that trigger bone resorption.[87] Thus, removing *P. gingivalis* may stop the inflammatory response leading to tissue destruction.[4] While the potential efficacy of PiezoGEL against other dental pathogens is promising, it is essential to recognize the need for further studies to validate its effects against various species commonly associated with oral infections. Future studies should evaluate the efficacy of PiezoGEL in periodontal red complex pathogens such as *Treponema denticola*, and *Tannerella forsythia*, to have a better understanding of possible microbial dynamics and microbiome changes derived from the biomaterial.

4.3. Bone-Tissue Regeneration Evaluation in Vitro. To explore the bone tissue regeneration of PiezoGEL, we

https://doi.org/10.1021/acsami.3c08336
ACS Appl. Mater. Interfaces XXXX, XXX, XXX−XXX

evaluated cell viability, osteogenic differentiation, and mineral formation after BMSCs were cultivated in hydrogels under static and loaded conditions for 7 and 14 days (Figure 3a).

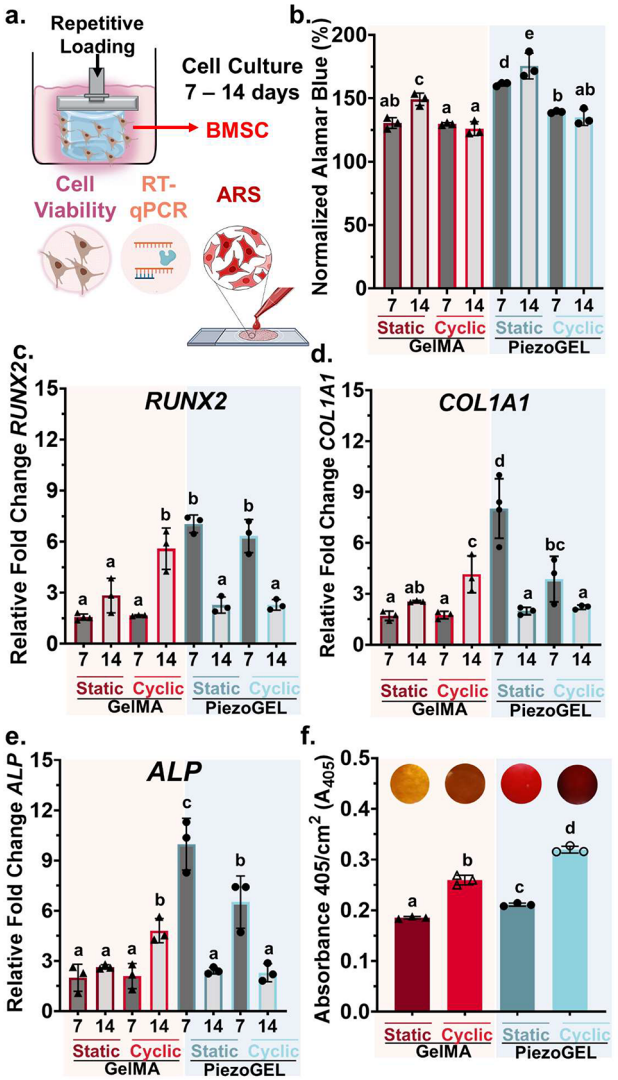

Figure 3. Osteogenic differentiation evaluation of GelMA and PiezoGEL hydrogels in vitro. (a) Schematics of the model developed to evaluate bone tissue regeneration on hydrogels subjected to cyclic mechanical loading and static (no loading). (b) Cell viability measured with alamarBlue reduction (%) and normalized with cells cultivated in an empty wells. Changes in the expression of selected genes related to osteoblast differentiation. (c) *RUNX2*, encoding runt-related transcription factor 2 required for intramembranous and endochondral bone development. (d) *COL1A1*, coding collagen type I. (e) *ALP*, encoding alkaline phosphatase. The relative gene expression was normalized to *GAPDH* (housekeeping). (f) Normalized absorbance values of Alizarin Red S staining of the formed ECM minerals formed after 14 days of cell culture. Mean values with different letters are significantly different ($p \leq 0.05$).

Overall, we observed a positive increase in cell viability of both hydrogel groups, indicating no cytotoxicity of these biomaterials (Figure 3b). The normalized reduction of alamarBlue >100% for all hydrogels (GelMA and PiezoGEL) indicates superior viability compared to that of the cells cultured in the empty well (reference used in normalization). Our results showed that the viability of PiezoGEL was significantly higher than that of GelMA for all evaluated days and loading conditions (Figure 3b). The results suggest that the addition of BTO positively affects cell proliferation. Interestingly, PiezoGEL under static conditions shows the highest viability. To explain this, we hypothesize that the cyclic mechanical stimulation of the PiezoGEL speeds up the biodegradation process due to the continuous movement forcing the additional leaching of BTO fillers, which reduces the electrical charge production (SI-12).

Looking into the expression of early markers of osteogenic differentiation, we examined relevant BMSC genes, including *RUNX2*, *COL1A1*, and *ALP*. The gene *RUNX2* is considered a master regulator of osteogenesis. It plays a crucial role in initiating the osteogenic differentiation process.[88] This gene was significantly upregulated by PiezoGEL on day 7 with a downregulation on day 14 (Figure 3c). The early expression of *RUNX2* indicates the quick degree of commitment and differentiation of BMSCs toward the osteoblast lineage and suggests the activation of other osteogenic genes and signaling pathways necessary for premature bone formation.[89] Interestingly, the static PiezoGEL group (no piezoelectric charge generation) also showed early expression of *RUNX2*. It is known that BTO particles alone accelerate osteogenesis.[90] Similar to cell viability, the leaching of BTO particles in loaded PiezoGEL can influence the early differentiation process. In future studies, we need to deconvolute the effective effect of piezoelectric charges and BTO fillers on osteogenic differentiation. Overall, hydrogels of GelMA did not significantly upregulate *RUNX2*. However, GelMA under cyclic loading for 14 days showed a significant upregulation. Cyclic loading of biomaterials has shown to induce osteogenic differentiation of BMSCs via Wnt/β-catenin signaling pathway,[91,92] which stimulates the expression of *ALP* and *RUNX2*.[93] A similar trend was observed in the expression of *COL1A1* and *ALP*. *COL1A1* is the major component of the ECM in bone. Its early expression is upregulated during osteogenic differentiation and is crucial for bone matrix synthesis.[94] Under both static and cyclic loading conditions, PiezoGEL demonstrated early differentiation of *COL1A1* within 7 days (Figure 3d), indicating the production of the initial extracellular matrix (ECM) essential for bone formation. The upregulation of *COL1A1* in PiezoGEL is a downstream effect of the *RUNX2* activation, which triggers genes involved in osteoblast differentiation.[95] Notably, the upregulation of *COL1A1* at day 7 from the cyclic PiezoGEL was significantly lower than that from the static group. It appears that the electrical charge generation from the cyclic loading accelerated the upregulation of early osteogenic gene expression. Genes' analysis at early time points (days 1 and 3) could explain this phenomenon. *ALP* is an enzyme that is highly expressed during osteogenic differentiation, and its expression increases as BMSCs differentiate into preosteoblasts and osteoblasts. *ALP* is involved in mineralization.[94] The gene expression trend between *ALP* and *RUNX2* is similar. For PiezoGEL, there is higher upregulation at day 7, whereas there was no regulation for GelMA (Figure 3e). *ALP* expression on day 7 suggests early osteoblast maturation and bone formation. However, as the bone formation process progresses, the activity of *ALP* may decrease as osteoblasts mature and mineralize the bone matrix.

Taken together, PiezoGEL induced the early expression of critical markers of bone formation, suggesting a quick osteogenic differentiation. Both piezoelectric charges and BTO fillers may be contributing to these responses. BTO

https://doi.org/10.1021/acsami.3c08336
ACS Appl. Mater. Interfaces XXXX, XXX, XXX−XXX

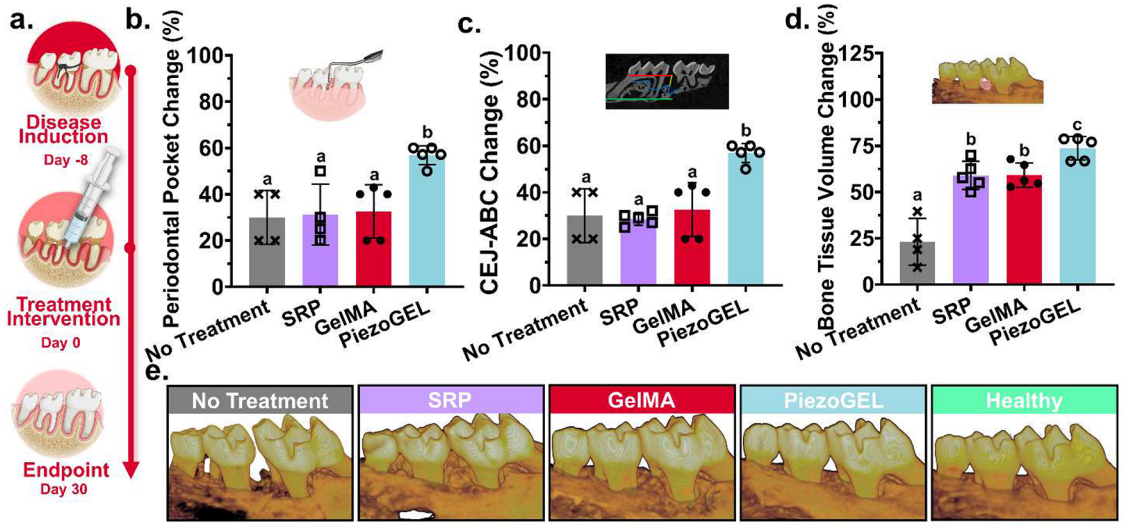

Figure 4. Periodontal bone tissue regeneration evaluations in vivo. (a) Schematic representation of the ligature-induced model in mice. A 5−0 silk ligature was tied around the maxillary second molar for 8 days to induce periodontitis. Bone regeneration was evaluated after 30 days of treatment. Treatment groups included scaling and root planning (SRP) as clinical reference, and SRP followed by the injection of both GelMA or PiezoGEL hydrogels. (b) Change of periodontal pocket depth calculated by measuring the before and after. (c) Change in cementum-enamel junction (CEJ) to alveolar bone crest (ABC) distance (yellow line). (d) Change in bone volume measured between molars 1 and 2 (ligature location) and quantified along several cut planes along the apical/occlusal direction. (e) Reconstructed 3D micro-CT images of the maxillary alveolar bone viewed from the lingual direction in all groups. Mean values with different letters are significantly different ($p \leq 0.05$).

generates electrical charges in response to mechanical stress.[97] This electrical charge stimulates BMSC to differentiate, proliferate, and form new bone tissue. Electrical charge can also stimulate angiogenesis necessary for bone regeneration.[96] Electric charges are known to affect cell behavior, including growth, migration, and differentiation.[97] These charges can stimulate the differentiation of stem cells into specific types of cells, such as bone-type cells, by influencing the flow of ions across the cell membrane, which activates signaling pathways involved in cell differentiation.[98,99] This is the first attempt to use piezoelectrical charges for periodontal bone tissue regeneration. BMSCs have been studied extensively for periodontal bone tissue regeneration due to the multilineage differentiation potential, are easily accessible, and exhibit a higher growth capacity than PDL cells.[100]

To study late-stage markers of bone formation, we evaluated the ECM mineralization at day 14.[101] A significant amount of mineral was noted for all of the hydrogels (Figure 3f). Specifically, cyclic PiezoGEL hydrogels exhibited the highest level of ECM mineralization, followed by the cyclic GelMA group. The lowest ECM mineralization was measured for the static GelMA group. These results are consistent with those showing the expression of *ALP* (Figure 3e), indicating that hydrogels under cyclic strain induced an early expression. In addition, ECM mineralization from PiezoGEL explains why the expression of *RUNX2*, *COL1A1*, and *ALP* on day 14 was not upregulated since it is possible that the peaks in expression occurred prior. In addition, ECM of interest, GelMA exhibited ECM mineralization which is consistent with previous reports.[102]

4.4. Periodontal Bone Regeneration and Inflammatory Evaluations in Vivo. PD and bone loss were successfully induced in mice after placing a ligature around the molars for a week. An initial clinical evaluation for bleeding and PD confirmed the induction of the disease for all the groups. Healthy and diseased pocket depths were 0.2 and 0.55 mm, respectively. In addition, micro-CT evaluation showed a distance between the CEJ and ABC for healthy and diseased animals of 0.18 mm and 0.60 mm, respectively (SI-13). Our results agree with previous studies showing that the pocket depth after 1 week of ligature-induced PD is ∼0.60 mm.[103] No adverse reactions, such as local/systemic toxic symptoms or weight loss, were observed during treatment. After 1 month of treatment, we evaluated changes in pocket depth, bone tissue, and inflammation. PiezoGEL showed the highest change in pocket depth among all other evaluated groups (Figure 4b). The final pocket size obtained for PiezoGEL after treatment was 0.2 mm, which is comparable to that under healthy conditions (SI-13). The pocket depth changes for GelMA, SRP, and no treatment were similar. These results are expected since no bioactive therapies were provided in these groups. The robust immune response and natural regenerative abilities of mice may explain why the no treatment group rendered similar pocket depth change.[104] Looking into the CEJ to ABC distance, again, PiezoGEL showed the highest change among other groups (Figure 4c). In other words, more bone tissue was regenerated after treatment. These results indicate that increased bone tissue regenerated by PiezoGEL helped reduce the size of the pocket and, thus, rendered a bigger change after treatment. GelMA, SRP, and no treatment groups showed a similar amount of regenerated bone and 50% less than PiezoGEL. Looking into the regenerated bone tissue volume, PiezoGEL showed the highest change among the other groups (Figure 4d). The no treatment group showed the lowest bone volume (20%), indicating the lowest amount of bone regeneration. The SRP and GelMA groups showed a similar amount of regenerated bone volume (55%), which was higher than no treatment but lower than PiezoGEL. Taken all together, these results indicate that PiezoGEL can augment bone tissue around the periodontium and reduce the pocket size without the need of surgery, bone grafts, or guided membranes. The 3D reconstruction of the maxilla for all groups confirmed previous observations (Figure 4e). Improved bone tissue quality and regeneration were observed for

https://doi.org/10.1021/acsami.3c08336
ACS Appl. Mater. Interfaces XXXX, XXX, XXX−XXX

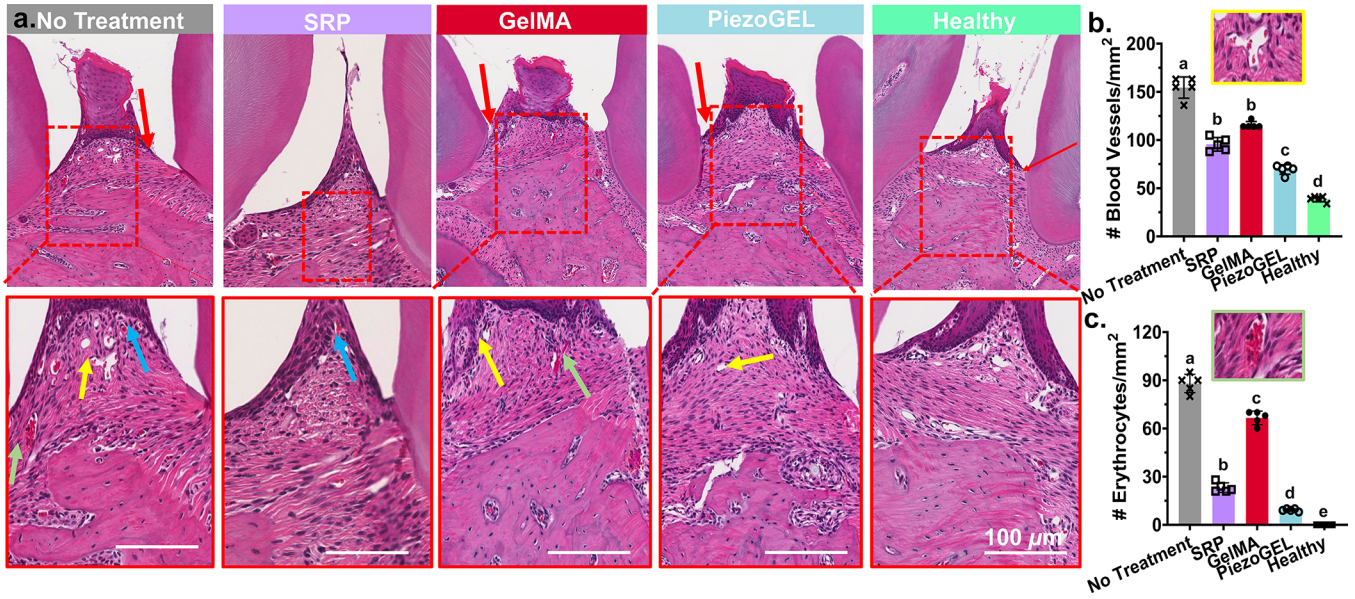

Figure 5. Histological evaluation of animal periodontal tissues. (a) Hematoxylin and eosin (H&E) images of periodontal tissue sections between the maxilla's first and second molars with magnification inset. (b) Number of blood vessels and (c) erythrocytes quantified in the regenerated area. The red arrow corresponds to epithelium detached from cement. Yellow arrows correspond to indicate blood vessels. Green and blue arrows correspond to erythrocytes and neutrophils, respectively.

PiezoGEL around M1−M2 (location of the defect). These qualities are comparable to those in healthy conditions. No treatment and GelMA showed the poorest bone tissue quality. Different studies have used GelMA as a carrier of bioactive biomaterials for periodontal bone tissue regeneration, including ZIF8,[27] hydroxyapatite,[105] bioactive glass[105], and BMP2 (bone morphogenetic protein 2).[105] These biomaterials establish a suitable microenvironment around the periodontal tissues and enable the delivery of bioactive therapy to promote bone regeneration.

Histological sections stained with H&E were used to evaluate the inflammatory response, cell infiltration, and morphological changes in periodontal tissues caused by PiezoGEL. Histopathological changes were used to evaluate the effectiveness of PiezoGEL in reducing bacterial load and infection in the tissue. The results of H&E staining supported the trends observed by micro-CT (Figure 5). In general, PD shows changes in epithelial detachment, epithelial hyperplasia, disorganization of collagen fibers, and erythrocyte density.[106] We looked for these features in all of the evaluated groups. Significant tissue destruction associated with chronic inflammation was observed in the GelMA and no treatment groups, while PiezoGEL and healthy groups showed, in general, a junctional epithelial union (red arrow, Figure 5a). Additionally, PiezoGEL and healthy groups showed decreased epithelial length (SI-9), inflammatory assessment, and lymphoplasmic infiltrate (SI-10a). The inflammatory response was quantified by counting the number of blood vessels (yellow arrows) and erythrocytes (green arrows) in the infected area between M1 and M2 (insets in Figure 5a). A higher number of blood vessels was counted in the no treatment group (~160 blood vessels/mm^2), followed by GelMA (~120 blood vessels/mm^2) (Figure 5b). Lower blood vessel count was found in the healthy (~40 blood vessels/mm^2) and PiezoGEL groups (73 blood vessels/mm^2). A higher number of blood vessels is associated with an ongoing inflammatory process in which new blood vessels are formed to supply oxygen and nutrients to the affected area.[107]

In PD, the increased number of blood vessels is often accompanied by the influence of immune cells such as neutrophils (blue arrows in insets of Figure 5a), which exacerbate the inflammatory response and lead to tissue destruction.[108] Dogs with PD showed an average number of blood vessels per mm^2 of 128, whereas it was 63 for treated (cured) tissues.[109] These counts agree with our current findings. Similar to the number of blood vessels, a low number of erythrocytes is associated with healthy periodontal tissues. In this study, lower erythrocyte counts were observed in the healthy and PiezoGEL groups (Figure 5c). Higher counts of erythrocytes were observed in the untreated group. A higher red blood cell count indicates increased vascular permeability and blood flow in the affected area, which can result from an inflammatory response and tissue damage.[107] Overall, our results indicated that PiezoGEL was able to decrease inflammation compared to healthy tissues. PiezoGEL successfully achieved clinical attachment level by improving pocket depth and recovering lost bone volume. Evaluation of these parameters is known to determine the success of periodontal regenerative therapy.[105]

The current standard of care for the nonsurgical treatment of PD includes SRP in combination with adjuvants (i.e., antibacterial agents).[110,111] However, clinically SRP fails to reduce the pocket size owing to insufficient antibacterial effects and the lack of natural regeneration of periodontal tissues.[112] Additionally, surgical approaches due to their high cost and invasiveness are limited to severe periodontitis. Recently, hydrogels have been used to treat PD because of their ability to encapsulate and release therapeutic agents in a controlled manner.[114] However, one of the major challenges for these hydrogels in treating PD is the need to effectively deliver combined antibacterial agents and regenerative therapies to the site of infection. Our hydrogel exhibits unique advantages as a single-use material in reaching periodontal defects and adapting to its shape, while providing dual antibacterial and regenerative effects. Bioactive therapies are provided using

https://doi.org/10.1021/acsami.3c08336
ACS Appl. Mater. Interfaces XXXX, XXX, XXX−XXX

nonleaching technologies, which can overcome the limitations of current technologies. There are several advantages of PiezoGEL over the current standards of care. First, the technology is fundamentally different from existing adjuvants and treatments for PD since it offers a drug-free antibacterial treatment without raising concerns regarding bacterial antibiotic resistance. Second, PiezoGEL has a simple formulation with only three ingredients: GelMA (a common hydrogel approved for medical use),[113] piezoelectric fillers, and a photoinitiator. We harness the benefits of hydrogels (injectable, light curable, conforms to pocket spaces, and biocompatibility) for delivery into the periodontal pocket. Third, PiezoGEL offers bone tissue regeneration without surgery, which is a novel concept in the nonsurgical treatment of PD. Some of the potential limitations of PiezoGEL are the possible short residency if the adhesion is poor and the control of the electrical charges to elicit therapies. The surgical treatment of PD from a biomaterials perspective relies on bone grafts, guided tissue regeneration (GTR), and tissue engineering with controlled delivery of drugs or growth factors.[111] Surgical approaches are invasive, technically challenging, with a high cost, and usually recommended when nonsurgical approaches are exhausted.

Findings from this work begin to pave the way for the clinical use of PiezoGEL in treating periodontitis. To translate the technology, future studies should consider additional biocompatibility tests based on ISO-10993, including oral toxicity, systemic toxicity, oral mucosal irrigation, and USP pyrogen. In addition, studying the adhesion of the hydrogel inside the pocket in vivo to determine the number of applications required for treatment is warranted. Also, additional degradation tests in vivo are required to explore the range of applications necessary for various patient populations and the severity of PD. Overall, PiezoGEL represents a significant advancement in PD treatment and holds great promise for improving patient outcomes in periodontal regenerative medicine.

5. CONCLUSIONS

In this study, we successfully developed an injectable piezoelectric hydrogel (PiezoGEL) for the nonsurgical treatment of periodontal disease by combining GelMA with barium titanate fillers. PiezoGEL exhibited remarkable antibacterial and bone-regeneration effects both vitro and in vivo. For antibacterial evaluations, PiezoGEL demonstrated a significant reduction in biofilm formation and viable cells against *P. gingivalis* compared to GelMA hydrogels in vitro. Moreover, PiezoGEL upregulated the expression of osteogenesis-related genes (*RUNX2*, *COL1A1*, and *ALP*) and promoted early ECM mineralization. In vivo, PiezoGEL relieved inflammation, promoted alveolar bone tissue regeneration, and reduced the periodontal pocket depth after 1 month of treatment. Results from both our in vitro and in vivo investigations strongly supported the efficacy of PiezoGEL as a promising bioactive material for the treatment of periodontal disease by combining antibacterial properties, osteogenic potential, and the ability to reduce inflammation.

■ ASSOCIATED CONTENT

Data Availability Statement

Research data supporting this study is available. Additional relevant data are presented in the Supporting Information.

Supporting Information

The Supporting Information is available free of charge at https://pubs.acs.org/doi/10.1021/acsami.3c08336.

Experimental details and methods (PDF)

■ AUTHOR INFORMATION

Corresponding Author

Santiago Orrego − *Department of Oral Health Sciences, Kornberg School of Dentistry, Temple University, Philadelphia, Pennsylvania 19140, United States; Bioengineering Department, College of Engineering, Temple University, Philadelphia, Pennsylvania 19122, United States;* orcid.org/0000-0003-3683-6750; Phone: +1-215-707-3817; Email: sorrego@temple.edu

Authors

Lina Roldan − *Department of Oral Health Sciences, Kornberg School of Dentistry, Temple University, Philadelphia, Pennsylvania 19140, United States; Bioengineering Research Group (GIB), Universidad EAFIT, Medellín 050037, Colombia*

Carolina Montoya − *Department of Oral Health Sciences, Kornberg School of Dentistry, Temple University, Philadelphia, Pennsylvania 19140, United States*

Varun Solanki − *Department of Oral Health Sciences, Kornberg School of Dentistry, Temple University, Philadelphia, Pennsylvania 19140, United States*

Kathy Q. Cai − *Histopathology Facility, Fox Chase Cancer, Temple University, Philadelphia, Pennsylvania 19140, United States*

Maobin Yang − *Department of Oral Health Sciences, Kornberg School of Dentistry and Department of Endodontology, Kornberg School of Dentistry, Temple University, Philadelphia, Pennsylvania 19140, United States*

Santiago Correa − *Bioengineering Research Group (GIB), Universidad EAFIT, Medellín 050037, Colombia*

Complete contact information is available at: https://pubs.acs.org/10.1021/acsami.3c08336

Author Contributions

Lina Roldan conducted all the in vitro tests for antibacterial activity and bone tissue regeneration. She planned, coordinated, and performed in vivo tests. She contributed to the writing process by drafting, reviewing, and editing of the manuscript. Carolina Montoya played a crucial role in the project, performing characterizations and in vivo tests, conceptualizing the study design, and contributing to the manuscript by writing, reviewing, and editing. Varun Solanki served as a clinician and helped perform the procedure on mice. Kathy Q. Cai conducted all the histological processing. Maobin Yang was instrumental in the experimental design and editing of the manuscript. Santiago Correa supervised the project and provided edits and feedback. Santiago Orrego provided the original idea for this project. He supervised the project, contributed to the conceptualization of the study design, secured funding, and was responsible for the project administration. He contributed to the writing process by drafting, reviewing, and editing the manuscript. He also helped conduct in vivo tests.

Funding

This study was supported by Temple University Maurice Kornberg School of Dentistry start-up fund, the Provost's

Office at Temple University Strategic Fund, and the University City Science Center's under the QED Proof-of-Concept Program Round 13.

Notes

The authors declare the following competing financial interest(s): S. Orrego and C. Montoya are affiliated with Oral Biolife, Inc.

■ ACKNOWLEDGMENTS

We thank Dr. Riya Kuklani, Mamta Amin, and Dr. Dmitriy A. Dikin from Temple University for their expertise and assistance during the histological analysis, micro-CT scanning, SEM evaluations, respectively. We express our gratitude to Dr. Julian David Muñoz, a pathologist from Universidad de Antioquia, Medellín, Colombia, for providing his valuable expertise in the evaluation of histological images in this study. Also, we acknowledge the support of Dr. Todd Abrahams and Niall Sweeny for their invaluable contributions and collaboration during this project's execution.

■ REFERENCES

(1) Eke, P. I.; Thornton-Evans, G. O.; Wei, L.; Borgnakke, W. S.; Dye, B. A.; Genco, R. J. Periodontitis in US adults: National health and nutrition examination survey 2009−2014. *Journal of the American Dental Association.* **2018**, *149*, 576−588.

(2) Socransky, S. S.; Haffajee, A. D.; Cugini, M. A.; Smith, C.; Kent, R. L. Microbial complexes in subgingival plaque. *J. Clin Periodontol.* **1998**, *25*, 134−144.

(3) Fi, C.; Wo, W. Periodontal disease and systemic diseases: An overview on recent progresses. *J. Biol. Regul Homeostatic Agents* **2021**, *35*, 1−9 (https://europepmc.org/article/med/33463138; accessed May 17, 2023).

(4) Jepsen, K.; Jepsen, S. Antibiotics/antimicrobials: Systemic and local administration in the therapy of mild to moderately advanced periodontitis. *Periodontol. 2000* **2016**, *71* (71), 82−112.

(5) Graziani, F.; Karapetsa, D.; Alonso, B.; Herrera, D. Nonsurgical and surgical treatment of periodontitis: How many options for one disease? *Periodontol. 2000* **2017**, *75* (1), 152−188.

(6) Darby, I. Non-surgical management of periodontal disease. *Aust Dent J.* **2009**, *54*, S86−S95.

(7) Soysa, N. S.; Waidyarathne, H.; Ranaweera, M.; Alles, C. N. R. A. Clinical efficacy of local application of sustained-release metronidazole in periodontal therapy. *Dent. Rev.* **2021**, *1*, No. 100006.

(8) Corbella, S.; Calciolari, E.; Alberti, A.; Donos, N.; Francetti, L. Systematic review and meta-analysis on the adjunctive use of host immune modulators in non-surgical periodontal treatment in healthy and systemically compromised patients. *Sci. Rep.* **2021**, *11*, 1−18.

(9) Ardila, C.-M.; Bedoya-García, J.-A.; Arrubla-Escobar, D.-E. Antibiotic resistance in periodontitis patients: A systematic scoping review of randomized clinical trials. *Oral Dis* **2022**, DOI: 10.1111/odi.14288.

(10) Davey, M. E.; O'toole, G. A. Microbial biofilms: From ecology to molecular genetics. *Microbiol Mol. Biol. Rev.* **2000**, *64*, 847−867.

(11) Iviglia, G.; Kargozar, S.; Baino, F. Biomaterials, current strategies, and novel nano-technological approaches for periodontal regeneration. *J. Funct. Biomater.* **2019**, *10*, 3.

(12) Bartold, P.; Gronthos, S.; Ivanovski, S.; Fisher, A.; Hutmacher, D. Tissue engineered periodontal products. *J. Periodontal Res.* **2016**, *51*, 1−15.

(13) Ribeiro, F. V.; Mehta, J. J.; Monteiro, M. F.; Moore, J.; Casati, M. Z.; Nibali, L. Minimal invasiveness in nonsurgical periodontal therapy. *Periodontol. 2000* **2023**, *91*, 7−19.

(14) Hernández-Monjaraz, B.; Santiago-Osorio, E.; Monroy-García, A.; Ledesma-Martínez, E.; Mendoza-Núñez, V. M. Mesenchymal stem cells of dental origin for inducing tissue regeneration in periodontitis: A mini-review. *Int. J. Mol. Sci.* **2018**, *19*, 944.

(15) Larsson, L.; Decker, A. M.; Nibali, L.; Pilipchuk, S. P.; Berglundh, T.; Giannobile, W. V. Regenerative medicine for periodontal and peri-implant diseases. *J. Dent Res.* **2016**, *95*, 255−266.

(16) Bonito, A. J.; Lux, L.; Lohr, K. N. Impact of local adjuncts to scaling and root planing in periodontal disease therapy: A systematic review. *J. Periodontol.* **2005**, *76*, 1227−1236.

(17) Shue, L.; Yufeng, Z.; Mony, U. Biomaterials for periodontal regeneration: A review of ceramics and polymers. *Biomatter.* **2012**, *2*, 271−277.

(18) Alonso, J. M.; Del Olmo, J. A.; Gonzalez, R. P.; Saez-martinez, V. Injectable hydrogels: From laboratory to industrialization. *Polymers (Basel)* **2021**, *13*, 650.

(19) Dong, Z.; Sun, Y.; Chen, Y.; Liu, Y.; Tang, C.; Qu, X. Injectable adhesive hydrogel through a microcapsule cross link for periodontitis treatment. *ACS Appl. Bio Mater.* **2019**, *2*, 5985−5994.

(20) Patrick, M. D.; Keys, J. F.; Kumar, H. S.; Annamalai, R. T. Injectable nanoporous microgels generate vascularized constructs and support bone regeneration in critical-sized defects. *Sci. Rep.* **2022**, *12*, 15811.

(21) Ribeiro, J. S.; Bordini, E. A. F.; Ferreira, J. A.; Mei, L.; Dubey, N.; Fenno, J. C.; Piva, E.; Lund, R. G.; Schwendeman, A.; Bottino, M. C. Injectable MMP-Responsive Nanotube-Modified Gelatin Hydrogel for Dental Infection Ablation. *ACS Appl. Mater. Interfaces.* **2020**, *12*, 16006−16017.

(22) Li, S.; Dong, S.; Xu, W.; Tu, S.; Yan, L.; Zhao, C.; Ding, J.; Chen, X. *Antibacterial Hydrogels* **2018**, *5*, No. 1700527.

(23) Ribeiro, J. S.; Daghrery, A.; Dubey, N.; Li, C.; Mei, L.; Fenno, J. C.; Schwendeman, A.; Aytac, Z.; Bottino, M. C. Hybrid antimicrobial hydrogel as injectable therapeutics for oral infection ablation. *Biomacromolecules.* **2020**, *21*, 3945−3956.

(24) Vargas-Alfredo, N.; Munar-Bestard, M.; Ramis, J.M.; Monjo, M. Synthesis and modification of gelatin methacryloyl (GelMA) with antibacterial quaternary groups and its potential for periodontal applications. *Gels* **2022**, *8*, 630.

(25) Shirzaei Sani, E.; Portillo Lara, R.; Aldawood, Z.; Bassir, S. H.; Nguyen, D.; Kantarci, A.; Intini, G.; Annabi, N. An antimicrobial dental light curable bioadhesive hydrogel for treatment of peri-implant diseases. *Matter.* **2019**, *1*, 926−944.

(26) Goto, R.; Nishida, E.; Kobayashi, S.; Aino, M.; Ohno, T.; Iwamura, Y.; Kikuchi, T.; Hayashi, J.-i.; Yamamoto, G.; Asakura, M.; Mitani, A. Gelatin methacryloyl-riboflavin (GelMA-rf) hydrogels for bone regeneration. *Int. J. Mol. Sci.* **2021**, *22*, 1635.

(27) Liu, Y.; Li, T.; Sun, M.; Cheng, Z.; Jia, W.; Jiao, K.; Wang, S.; Jiang, K.; Yang, Y.; Dai, Z.; Liu, L.; Liu, G.; Luo, Y. ZIF-8 modified multifunctional injectable photopolymerizable GelMA hydrogel for the treatment of periodontitis. *Acta Biomater.* **2022**, *146*, 37−48.

(28) Dubey, N.; Ferreira, J. A.; Daghrery, A.; Aytac, Z.; Malda, J.; Bhaduri, S. B.; Bottino, M. C. Highly tunable bioactive fiber-reinforced hydrogel for guided bone regeneration. *Acta Biomater.* **2020**, *113*, 164−176.

(29) Solovieva, A. B.; Rudenko, T. G.; Shekhter, A. B.; Glagolev, N. N.; Spokoinyi, A. L.; Fayzullin, A. L.; Aksenova, N. A.; Shpichka, A. I.; Kardumyan, V. V.; Timashev, P. S. Broad-spectrum antibacterial and pro-regenerative effects of photoactivated Photodithazine-Pluronic F127-Chitosan polymer system: In vivo study. *J. Photochem. Photobiol. B* **2020**, *210*, No. 111954.

(30) Huang, M.; Huang, Y.; Liu, H.; Tang, Z.; Chen, Y.; Huang, Z.; Xu, S.; Du, J.; Jia, B. Hydrogels for the treatment of oral and maxillofacial diseases: current research, challenges, and future directions. *Biomater Sci.* **2022**, *10*, 6413−6446.

(31) Li, M.; Lv, J.; Yang, Y.; Cheng, G.; Guo, S.; Liu, C.; Ding, Y. Advances of hydrogel therapy in periodontal regeneration-A materials perspective review. *Gels.* **2022**, *8*, 624.

(32) Lee, Y.; Gou, Y.; Pan, X.; Gu, Z.; Xie, H. Advances of multifunctional hydrogels for periodontal disease. *Smart Mater. Med.* **2023**, *4*, 460−467.

(33) Xu, X.; Gu, Z.; Chen, X.; Shi, C.; Liu, C.; Liu, M.; Wang, L.; Sun, M.; Zhang, K.; Liu, Q.; Shen, Y.; Lin, C.; Yang, B.; Sun, H. An injectable and thermosensitive hydrogel: Promoting periodontal

regeneration by controlled-release of aspirin and erythropoietin. *Acta Biomater.* **2019**, *86*, 235−246.
(34) Usui, M.; Onizuka, S.; Sato, T.; Kokabu, S.; Ariyoshi, W.; Nakashima, K. Mechanism of alveolar bone destruction in periodontitis — Periodontal bacteria and inflammation. *Japanese Dental Science Review.* **2021**, *57*, 201−208.
(35) Ramadan, D. E.; Hariyani, N.; Indrawati, R.; Ridwan, R. D.; Diyatri, I. Cytokines and chemokines in periodontitis., Eur. *J. Dent.* **2020**, *14*, 483.
(36) Zaszczyńska, A.; Gradys, A.; Sajkiewicz, P. Progress in the applications of smart piezoelectric materials for medical devices. *Polymers (Basel)* **2020**, *12*, 2754.
(37) Ribeiro, C.; Sencadas, V.; Correia, D. M.; Lanceros-Méndez, S. Piezoelectric polymers as biomaterials for tissue engineering applications. *Colloids Surf. B Biointerfaces.* **2015**, *136*, 46−55.
(38) Kao, F. C.; Chiu, P. Y.; Tsai, T. T.; Lin, Z. H. The application of nanogenerators and piezoelectricity in osteogenesis. *Sci. Technol. Adv. Mater.* **2019**, *20*, 1103−1117.
(39) Acosta, M.; Novak, N.; Rojas, V.; Patel, S.; Vaish, R.; Koruza, J.; Rossetti, G.A.; Rödel, J. BaTiO3-based piezoelectrics: Fundamentals, current status, and perspectives. *Appl. Phys. Rev.* **2017**, *4*, 041305.
(40) Zhang, Y.; Chen, L.; Zeng, J.; Zhou, K.; Zhang, D. Aligned porous barium titanate/hydroxyapatite composites with high piezoelectric coefficients for bone tissue engineering. *Materials Science and Engineering C* **2014**, *39*, 143−149.
(41) Ghosh, S.; Qiao, W.; Yang, Z.; Orrego, S.; Neelakantan, P. Engineering dental tissues using biomaterials with piezoelectric effect: Current progress and future perspectives. *J. Funct. Biomater.* **2023**, *14*, 8.
(42) Montoya, C.; Jain, A.; Londoño, J. J.; Correa, S.; Lelkes, P. I.; Melo, M. A.; Orrego, S. Multifunctional dental composite with piezoelectric nanofillers for combined antibacterial and mineralization effects. *ACS Appl. Mater. Interfaces.* **2021**, *13*, 43868−43879.
(43) Montoya, C.; Kurylec, J.; Baraniya, D.; Tripathi, A.; Puri, S.; Orrego, S. Antifungal effect of piezoelectric charges on PMMA dentures. *ACS Biomater Sci. Eng.* **2021**, *7*, 4838−4846.
(44) Valero, C.; Amaveda, H.; Mora, M.; García-Aznar, J. M. Combined experimental and computational characterization of crosslinked collagen-based hydrogels. *PLoS One.* **2018**, *13*, No. e0195820.
(45) González, G.; Baruffaldi, D.; Martinengo, C.; Angelini, A.; Chiappone, A.; Roppolo, I.; Pirri, C.F.; Frascella, F. Materials testing for the development of biocompatible devices through vat-polymerization 3d printing. *Nanomaterials (Basel)* **2020**, *10*, 1788.
(46) Moreira, C. D. F.; Carvalho, S. M.; Sousa, R. G.; Mansur, H. S.; Pereira, M. M. Nanostructured chitosan/gelatin/bioactive glass in situ forming hydrogel composites as a potential injectable matrix for bone tissue engineering. *Mater. Chem. Phys.* **2018**, *218*, 304−316.
(47) Yuan, H.; Chen, L.; Hong, F. F. A biodegradable antibacterial nanocomposite based on oxidized bacterial nanocellulose for rapid hemostasis and wound healing. *ACS Appl. Mater. Interfaces.* **2020**, *12*, 3382−3392.
(48) Sánchez, M. C.; Romero-Lastra, P.; Ribeiro-Vidal, H.; Llama-Palacios, A.; Figuero, E.; Herrera, D.; Sanz, M. Comparative gene expression analysis of planktonic Porphyromonas gingivalis ATCC 33277 in the presence of a growing biofilm versus planktonic cells. *BMC Microbiol.* **2019**, *19*, 58.
(49) How, K. Y.; Song, K. P.; Chan, K. G. Porphyromonas gingivalis: an overview of periodontopathic pathogen below the gum line. *Front. Microbiol.* **2016**, *7*, DOI: 10.3389/fmicb.2016.00053 (accessed November 11, 2021).
(50) Lian, D.; Dai, L.; Xie, Z.; Zhou, X.; Liu, X.; Zhang, Y.; Huang, Y.; Chen, Y. Periodontal ligament fibroblasts migration injury via ROS/TXNIP/Nlrp3 inflammasome pathway with Porphyromonas gingivalis lipopolysaccharide. *Mol. Immunol.* **2018**, *103*, 209−219.
(51) Mendez, K. N.; Hoare, A.; Soto, C.; Bugueño, I.; Olivera, M.; Meneses, C.; Pérez-Donoso, J. M.; Castro-Nallar, E.; Bravo, D. Variability in Genomic and Virulent Properties of Porphyromonas gingivalis Strains Isolated From Healthy and Severe Chronic Periodontitis Individuals. *Front Cell Infect Microbiol.* **2019**, *9*, 246.
(52) Nikolaus, A.; Currey, J. D.; Lindtner, T.; Fleck, C.; Zaslansky, P. Importance of the variable periodontal ligament geometry for whole tooth mechanical function: A validated numerical study. *J. Mech Behav Biomed Mater.* **2017**, *67*, 61−73.
(53) Yoshida, N.; Koga, Y.; Peng, C. L.; Tanaka, E.; Kobayashi, K. In vivo measurement of the elastic modulus of the human periodontal ligament. *Med. Eng. Phys.* **2001**, *23*, 567−572.
(54) Camilleri, J.; Arias Moliz, T.; Bettencourt, A.; Costa, J.; Martins, F.; Rabadijeva, D.; Rodriguez, D.; Visai, L.; Combes, C.; Farrugia, C.; Koidis, P.; Neves, C. Standardization of antimicrobial testing of dental devices. *Dental Materials.* **2020**, *36*, e59−e73.
(55) Sharaf, S.; Hijazi, K. Modulatory Mechanisms of Pathogenicity in Porphyromonas gingivalis and Other Periodontal Pathobionts. *Microorganisms* **2023**, *11*, 15.
(56) Romero-Lastra, P.; Sánchez, M. C.; Llama-Palacios, A.; Figuero, E.; Herrera, D.; Sanz, M. Gene expression of Porphyromonas gingivalis ATCC 33277 when growing in an in vitro multispecies biofilm. *PLoS One* **2019**, *14*, e0221234.
(57) Rao, X.; Huang, X.; Zhou, Z.; Lin, X. An improvement of the 2^(delta delta CT) method for quantitative real-time polymerase chain reaction data analysis. *Biostat. Bioinf. Biomath.* **2013**, *3*, 71 (accessed May 17, 2023).
(58) Raju, R.; Oshima, M.; Inoue, M.; Morita, T.; Huijiao, Y.; Waskitho, A.; Baba, O.; Inoue, M.; Matsuka, Y. Three-dimensional periodontal tissue regeneration using a bone-ligament complex cell sheet. *Sci. Rep.* **2020**, *10*, 1−16.
(59) Invitrogen, alamarBlue HS Cell Viability Reagent, 2019, 1−2.
(60) Posimo, J. M.; Unnithan, A. S.; Gleixner, A. M.; Choi, H. J.; Jiang, Y.; Pulugulla, S. H.; Leak, R. K. Viability assays for cells in culture. *J. Vis Exp.* **2014**, No. e50645.
(61) Svec, D.; Andersson, D.; Pekny, M.; Sjöback, R.; Kubista, M.; Ståhlberg, A. Direct cell lysis for single-cell gene expression profiling. *Front. Oncol.* **2013**, *3*, 1−11.
(62) Stephens, A. S.; Stephens, S. R.; Morrison, N. A. Internal control genes for quantitative RT-PCR expression analysis in mouse osteoblasts, osteoclasts and macrophages. *BMC Res. Notes.* **2011**, *4*, 410.
(63) Hatt, L.P.; Thompson, K.; Müller, W. E. G.; Stoddart, M.J.; Armiento, A.R. Calcium polyphosphate nanoparticles act as an effective inorganic phosphate source during osteogenic differentiation of human mesenchymal stem cells. *Int. J. Mol. Sci.* **2019**, *20*, 5801.
(64) Moser, C.; Bardsley, K.; El Haj, A. J., Alini, M.; Stoddart, M. J.; Bara, J. J. A perfusion culture system for assessing bone marrow stromal cell differentiation on PLGA scaffolds for bone repair. *Front. Bioeng. Biotechnol.* **2018**, *6*, DOI: 10.3389/fbioe.2018.00161.
(65) Tsukasaki, M.; Komatsu, N.; Nagashima, K.; Nitta, T.; Pluemsakunthai, W.; Shukunami, C.; Iwakura, Y.; Nakashima, T.; Okamoto, K.; Takayanagi, H. Host defense against oral microbiota by bone-damaging T cells. *Nat. Commun.* **2018**, *9*, 1−11.
(66) Marchesan, J.; Girnary, M. S.; Jing, L.; Miao, M. Z.; Zhang, S.; Sun, L.; Morelli, T.; Schoenfisch, M. H.; Inohara, N.; Offenbacher, S.; Jiao, Y. An experimental murine model to study periodontitis. *Nat. Protoc.* **2018**, *13*, 2247−2267.
(67) de Molon, R. S.; Park, C. H.; Jin, Q.; Sugai, J.; Cirelli, J. A. Characterization of ligature-induced experimental periodontitis. *Microsc Res. Technol.* **2018**, *81*, 1412−1421.
(68) Bouxsein, M. L.; Boyd, S. K.; Christiansen, B. A.; Guldberg, R. E.; Jepsen, K. J.; Müller, R. Guidelines for assessment of bone microstructure in rodents using micro-computed tomography., Journal of Bone and Mineral. *Research.* **2010**, *25*, 1468−1486.
(69) Zong, C.; Van Dessel, J.; Vande Velde, G.; Willems, G.; Cadenas de Llano-Pérula, M. Dynamic changes in tooth displacement and bone morphometry induced by orthodontic force. *Sci. Rep.* **2022**, *12*, 1−13.
(70) Chavez, M. B.; Chu, E. Y.; Kram, V.; de Castro, L. F.; Somerman, M. J.; Foster, B. L. Guidelines for Micro-Computed

Tomography Analysis of Rodent Dentoalveolar Tissues. *JBMR Plus* **2021**, *5*, DOI: 10.1002/jbm4.10474.
(71) Batool, F.; Strub, M.; Petit, C.; Bugueno, I.M.; Bornert, F.; Clauss, F.; Huck, O.; Kuchler-Bopp, S.; Benkirane-Jessel, N. Periodontal tissues, maxillary jaw bone, and tooth regeneration approaches: From animal models analyses to clinical applications. *Nanomaterials* **2018**, *8*, 337.
(72) Chen, Y.; Yang, Q.; Lv, C.; Chen, Y.; Zhao, W.; Li, W.; Chen, H.; Wang, H.; Sun, W.; Yuan, H. NLRP3 regulates alveolar bone loss in ligature-induced periodontitis by promoting osteoclastic differentiation. *Cell Prolif.* **2021**, *54*, e12973.
(73) Lin, J.; He, Z.; Liu, F.; Feng, J.; Huang, C.; Sun, X.; Deng, H. Hybrid Hydrogels for Synergistic Periodontal Antibacterial Treatment with Sustained Drug Release and NIR-Responsive Photothermal Effect. *Int. J. Nanomedicine.* **2020**, *15*, 5377.
(74) Kim, G.-T.; Go, H.-B.; Yu, J.-H.; Yang, S.-Y.; Kim, K.-M.; Choi, S.-H.; Kwon, J.-S. Cytotoxicity, colour stability and dimensional accuracy of 3d printing resin with three different photoinitiators. *Polymers (Basel)* **2022**, *14*, 979.
(75) Gorsche, C.; Harikrishna, R.; Baudis, S.; Knaack, P.; Husar, B.; Laeuger, J.; Hoffmann, H.; Liska, R. Real Time-NIR/MIR-Photorheology: A Versatile Tool for the in Situ Characterization of Photopolymerization Reactions. *Anal. Chem.* **2017**, *89*, 4958−4968.
(76) Heltmann-Meyer, S.; Steiner, D.; Müller, C.; Schneidereit, D.; Friedrich, O.; Salehi, S.; Engel, F.B.; Arkudas, A.; Horch, R.E. Gelatin methacryloyl is a slow degrading material allowing vascularization and long-term use in vivo. *Biomed. Mater. (Bristol)* **2021**, *16*, 065004.
(77) Carvalho, E. O.; Fernandes, M. M.; Padrao, J.; Nicolau, A.; Marqués-Marchán, J.; Asenjo, A.; Gama, F. M.; Ribeiro, C.; Lanceros-Mendez, S. Tailoring bacteria response by piezoelectric stimulation. *ACS Appl. Mater. Interfaces.* **2019**, *11*, 27297−27305.
(78) Lin, X.; Wu, J.; Xie, H. Porphyromonas gingivalis minor fimbriae are required for cell-cell interactions. *Infect. Immun.* **2006**, *74*, 6011−6015.
(79) Lamont, R. J.; Jenkinson, H. F. Subgingival colonization by Porphyromonas gingivalis. *Oral Microbiol Immunol.* **2000**, *15*, 341−349.
(80) Storz, G.; Tartaglia, L. A. OxyR: A regulator of antioxidant genes. *J. Nutr.* **1992**, *122*, 627−630.
(81) Wu, J.; Lin, X.; Xie, H. OXYR is involved in coordinate regulation of expression of FIMA and SOD genes in Porphyromonas gingivalis. *FEMS Microbiol Lett.* **2008**, *282*, 188−195.
(82) Meuric, V.; Gracieux, P.; Tamanai-Shacoori, Z.; Perez-Chaparro, J.; Bonnaure-Mallet, M. Expression patterns of genes induced by oxidative stress in Porphyromonas gingivalis. *Oral Microbiol Immunol.* **2008**, *23*, 308−314.
(83) Wang, G.; Tang, K.; Jiang, W.; Liao, Q.; Li, Y.; Liu, P.; Wu, Y.; Liu, M.; Wang, H.; Li, B.; Du, J.; Chu, P. K. Quantifiable relationship between antibacterial efficacy and electro-mechanical intervention on nanowire arrays. *Adv. Mater.* **2023**, *35*, No. e2212315.
(84) Zou, P.; Cao, P.; Liu, J.; Li, P.; Luan, Q. Comparisons of the killing effect of direct current partially mediated by reactive oxygen species on Porphyromonas gingivalis and Prevotella intermedia in planktonic state and biofilm state - an in vitro study. *J. Dent Sci.* **2022**, *17*, 459−467.
(85) Yamamoto, R.; Noiri, Y.; Yamaguchi, M.; Asahi, Y.; Maezono, H.; Ebisu, S. Time course of gene expression during Porphyromonas gingivalis strain ATCC 33277 biofilm formation. *Appl. Environ. Microbiol.* **2011**, *77*, 6733−6736.
(86) Juan, C.A.; de la Lastra, J. M. P.; Plou, F.J.; Pérez-Lebeña, E. The Chemistry of Reactive Oxygen Species (ROS) Revisited: Outlining Their Role in Biological Macromolecules (DNA, Lipids and Proteins) and Induced Pathologies. *Int. J. Mol. Sci.* **2021**, *22*, 4642.
(87) Ishida, N.; Ishihara, Y.; Ishida, K.; Tada, H.; Funaki-Kato, Y.; Hagiwara, M.; Ferdous, T.; Abdullah, M.; Mitani, A.; Michikawa, M.; Matsushita, K. Periodontitis induced by bacterial infection exacerbates features of Alzheimer's disease in transgenic mice. *NPJ. Aging Mech Dis.* **2017**, *3*, 1−7.
(88) Liu, T. M.; Lee, E. H. Transcriptional regulatory cascades in Runx2-dependent bone development. *Tissue Eng. Part B Rev.* **2013**, *19*, 254−263.
(89) Komori, T. Regulation of osteoblast differentiation by Runx2. *Adv. Exp. Med. Biol.* **2009**, *658*, 43−49.
(90) Furuya, K.; Morita, Y.; Tanaka, K.; Katayama, T.; Nakamachi, E. Acceleration of osteogenesis by using barium titanate piezoelectric ceramic as an implant material. *Proc. SPIE* **2011**, *7975*, 79750U.
(91) Liu, Y.; Cheng, W.; Zhao, Y.; Gao, L.; Chang, Y.; Tong, Z.; Li, H.; Jing, J. Cyclic Mechanical Strain Regulates Osteoblastic Differentiation of Mesenchymal Stem Cells on TiO_2 Nanotubes Through GCN5 and Wnt/β-Catenin. *Front. Bioeng. Biotechnol.* **2021**. *9*, DOI: 10.3389/fbioe.2021.735949.
(92) Lin, S.; Li, J.; Dong, L.; Cheng, K.; Lin, J.; Weng, W. Periodic-Mechanical-Stimulus Enhanced Osteogenic Differentiation of Mesenchymal Stem Cells on Fe3O4/Mineralized Collagen Coatings. *ACS Biomater Sci. Eng.* **2019**, *5*, 6446−6453.
(93) Krause, U.; Harris, S.; Green, A.; Ylostalo, J.; Zeitouni, S.; Lee, N.; Gregory, C. A. Pharmaceutical modulation of canonical Wnt signaling in multipotent stromal cells for improved osteoinductive therapy. *Proc. Natl. Acad. Sci. U. S. A.* **2010**, *107*, 4147−4152.
(94) Vimalraj, S. Alkaline phosphatase: Structure, expression and its function in bone mineralization. *Gene.* **2020**, *754*, No. 144855.
(95) Komori, T. Regulation of bone development and extracellular matrix protein genes by RUNX2. *Cell Tissue Res.* **2010**, *339*, 189−195.
(96) Leppik, L.; Oliveira, K. M. C.; Bhavsar, M. B.; Barker, J. H. Electrical stimulation in bone tissue engineering treatments. *European Journal of Trauma and Emergency Surgery.* **2020**, *46*, 231−244.
(97) Levin, M. Molecular bioelectricity: How endogenous voltage potentials control cell behavior and instruct pattern regulation in vivo. *Mol. Biol. Cell* **2014**, *25*, 3835−3850.
(98) Heng, B. C.; Bai, Y.; Li, X.; Meng, Y.; Zhang, X.; Deng, X. Signaling pathways implicated in enhanced stem/progenitor cell differentiation on electroactive scaffolds. *Smart Mater. Med.* **2022**, *3*, 4−11.
(99) Harris, M. P. Bioelectric signaling as a unique regulator of development and regeneration. *Development* **2021**, *148*, dev180794.
(100) Li, Q.; Yang, G.; Li, J.; Ding, M.; Zhou, N.; Dong, H.; Mou, Y. Stem cell therapies for periodontal tissue regeneration: A network meta-analysis of preclinical studies. *Stem Cell Res. Ther.* **2020**, *11*, 1−15.
(101) Hayashi, O.; Katsube, Y.; Hirose, M.; Ohgushi, H.; Ito, H. Comparison of osteogenic ability of rat mesenchymal stem cells from bone marrow, periosteum, and adipose tissue. *Calcif Tissue Int.* **2008**, *82*, 238−247.
(102) Shi, Z.; Xu, Y.; Mulatibieke, R.; Zhong, Q.; Pan, X.; Chen, Y.; Lian, Q.; Luo, X.; Shi, Z.; Zhu, Q. Nano-silicate-reinforced and sdf-1α-loaded gelatin-methacryloyl hydrogel for bone tissue engineering. *Int. J. Nanomedicine.* **2020**, *15*, 9337−9353.
(103) Li, D.; Feng, Y.; Tang, H.; Huang, L.; Tong, Z.; Hu, C.; Chen, X.; Tan, J. A Simplified and Effective Method for Generation of Experimental Murine Periodontitis Model. *Front. Bioeng. Biotechnol.* **2020**, *8*, 444.
(104) Masopust, D.; Sivula, C. P.; Jameson, S. C. Of mice, dirty mice, and men: Using mice to understand human immunology. *Journal of Immunology.* **2017**, *199*, 383−388.
(105) Chen, X.; Bai, S.; Li, B.; Liu, H.; Wu, G.; Liu, S.; Zhao, Y. Fabrication of gelatin methacrylate/nanohydroxyapatite microgel arrays for periodontal tissue regeneration. *Int. J. Nanomedicine.* **2016**, *11*, 4707−4718.
(106) Ionel, A.; Lucaciu, O.; Tăbăran, F.; Berce, C.; Toader, S.; Hurubeanu, L.; Bondor, C.; Câmpian, R. S. Histopathological and clinical expression of periodontal disease related to the systemic inflammatory response. *Histol. Histopathol.* **2017**, *32*, 379−384.
(107) Pahwa, R.; Goyal, A.; Jialal, I. *Chronic Inflammation*; StatPearls: Treasure Island, FL, 2023.
(108) Cortés-Vieyra, R.; Rosales, C.; Uribe-Querol, E. Neutrophil functions in periodontal homeostasis. *J. Immunol Res.* **2016**, *2016*, No. 1396106.

https://doi.org/10.1021/acsami.3c08336
ACS Appl. Mater. Interfaces XXXX, XXX, XXX−XXX

(109) Imber, J. C.; Roccuzzo, A.; Stähli, A.; Saulacic, N.; Deschner, J.; Sculean, A.; Bosshardt, D. D. Immunohistochemical evaluation of periodontal regeneration using a porous collagen scaffold. *Int. J. Mol. Sci.* **2021**, *22*, 10915.
(110) Khattri, S.; Kumbargere Nagraj, S.; Arora, A.; Eachempati, P.; Kusum, C. K.; Bhat, K. G.; Johnson, T. M.; Lodi, G. Adjunctive systemic antimicrobials for the non-surgical treatment of periodontitis. *Cochrane Database Syst. Rev.* **2020**, *11*, CD012568.
(111) Liang, Y.; Luan, X.; Liu, X. Recent advances in periodontal regeneration: A biomaterial perspective. *Bioact Mater.* **2020**, *5*, 297−308.
(112) Van der Weijden, G. A.; Dekkers, G. J.; Slot, D. E. Success of non-surgical periodontal therapy in adult periodontitis patients: A retrospective analysis. *Int. J. Dent Hyg.* **2019**, *17*, 309−317.
(113) Piao, Y.; You, H.; Xu, T.; Bei, H. P.; Piwko, I. Z.; Kwan, Y. Y.; Zhao, X. Biomedical applications of gelatin methacryloyl hydrogels. *Engineered Regeneration.* **2021**, *2*, 47−56.
(114) Ye, S.; Wei, B.; Zeng, L. Advances on hydrogels for oral science research. *Gels* **2022**, *8*, 302.

https://doi.org/10.1021/acsami.3c08336
ACS Appl. Mater. Interfaces XXXX, XXX, XXX−XXX